

Gated combo nanodevice for sequential operations on single electron spin

S. Bednarek and B. Szafran

Faculty of Physics and Applied Computer Science, AGH University of Science and Technology, al. Mickiewicza 30, 30-059 Kraków, Poland

Abstract.

An idea for a nanodevice in which an arbitrary sequence of three basic quantum single qubit gates - negation, Hadamard and phase shift - can be performed on a single electron spin. The spin state is manipulated using the spin-orbit coupling and the electron trajectory is controlled by the electron wave function self-focusing mechanism due to the electron interaction with the charge induced on metal gates. We present results of simulations based on iterative solution of the time dependent Schrödinger equation in which the subsequent operations on the electron spin can be followed and controlled. Description of the moving electron wave packet requires evaluation of the electric field within the entire nanodevice in each time step.

PACS numbers: 73.21.La, 73.63.Nm, 03.67.Lx

1. Introduction

The power which is in principle offered by the idea of the quantum computation stimulated an extensive effort toward realization of quantum gates. Several quantum systems are studied for application in encoding a quantum bit of information. The spin of an electron confined inside a semiconductor nanostructure is considered particularly promising [1, 2, 3]. A number of nanodevices were proposed and experimentally studied for operations on the electron spin [4, 5, 6, 7, 8]. For practical applications most useful are devices that function without microwave radiation and without external magnetic fields. An example of such a construction is the nanodevice presented in Ref. [8] in which the operations on the electron spin are performed using the spin-orbit coupling, and the transitions between the spin states are induced by AC voltages applied to the electrodes. The spin-orbit coupling can also be used for operations on the electron spins in opened quantum rings [9, 10]. In Ref. [9] a system of quantum rings is proposed for spin transformations according to three basic quantum gates: NOT, phase shift and Hadamard transform in a spin-dependent scattering experiment. In Ref. [10] a programable array of rings was proposed to split the incoming electron wave function is split into two parts each corresponding to an opposite spin orientation. In these papers [9, 10] time independent scattering problem is solved, with the electron spread all over the space with position dependent spin orientation. Recently, we proposed [12] a different device in which the position of the electron is localized in form of a wave packet which is self-focused by the interaction of the metal with the charge induced on the surface of metal electrodes which are deposited on top of the nanostructure and form induced quantum wires or induced quantum dots [11]. The electron localized in the wave packet has a definite spin orientation in every moment in time, and operation on the spin are performed by electron motion within the nanostructure. In contrast to the spin-dependent scattering approaches in open structures, the operations on the electron spin are performed in a compact nanodevice and result of time-evolution operators according to the original theory of quantum computation. In the proposed device [11] one can set the electron in motion along precise trajectories. Due to the interaction of the electron with the charge induced on the metal electrodes the electron wave function becomes self-focused [13, 14] forming a stable wave packet that can be directed to a chosen location within the nanostructure with probability 1.

Systems proposed in Ref. [12] exploit the Rashba coupling [16] in the absence of the Dresselhaus [15] coupling. They can be produced in semiconductors of the diamond structure, in Si or Ge for instance. A similar device working in III-V or II-VI material of zinc blende structure will work in presence of the Dresselhaus coupling resulting of inversion asymmetry of the crystal lattice. For both Rashba and Dresselhaus coupling present and y direction chosen in the growth direction the spin rotations with respect to the x and the z axes will occur for the electron moving in spatial directions within a plane of confinement (x, z) forming a narrow angle whose specific value depends on the the coupling constants. A practical realization of such a device is possible although more

challenging than the ones in which only one type of the spin-orbit coupling is present. In the present paper we assume that the quantum well in which the electron moves is perfectly symmetric so that the Rashba coupling constant is zero. Accordingly, we will consider the Dresselhaus coupling only. Then, the spin rotations around both the axes will be performed by electron moving in perpendicular spatial directions.

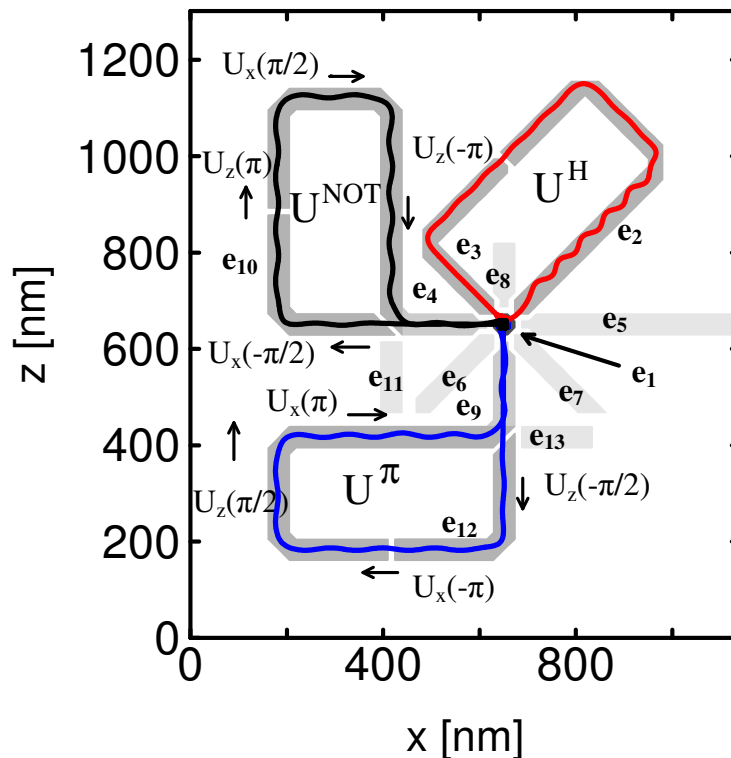


Figure 1. System of thirteen electrodes deposited on top of the planar semiconductor structure. The electrodes e_1, e_2, \dots, e_{13} are plotted in grey. A quantum dot induced under the electrode e_1 is used as the starting and the ending point of each trajectory. Trajectories of the electron at which its spin is subject to the negation U^{NOT} , phase shift U^π and Hadamard transform U^H are marked by black, blue and red curves, respectively.

2. Theory

Systems discussed below are based on a planar semiconductor structure as previously considered in Refs. [11, 12]. It contains a 10 nm wide quantum well sandwiched between tunnel barriers each 10 nm thick. The structure is separated of the strongly doped substrate by a undoped buffer layer 50 nm thick. On top of the other tunnel barrier metal electrodes are deposited. The electron gas within the electrodes is a source of the response potential which keeps the electron wave function in a form of a stable wave packet [13, 14] and sets its motion with a controlled trajectory by application of voltages [11]. The electron motion in the growth y direction is frozen by the confinement within

the quantum well. We use the following Hamiltonian:

$$H(x, z, t) = -\frac{\hbar^2}{2m} \left(\frac{\partial^2}{\partial x^2} + \frac{\partial^2}{\partial y^2} \right) - e\Phi(x, y_0, z, t) + H_D, \quad (1)$$

where y_0 is the center of the quantum well, and Φ is the electrostatic potential distribution inside the quantum well. This potential is evaluated in a three dimensional region containing the entire nanodevice by solution of the Poisson equation with the method described in detail in Ref. [11, 12]. The calculation method allows for description of the self-focusing effect [13] and the time dependence of the potential distribution during motion of the electron wave packet. The last term of the Hamiltonian (1) introduces the spin-orbit coupling by the Dresselhaus term

$$H_D = \frac{\hbar k_{so}}{m} (p_x \sigma_x - p_z \sigma_z), \quad (2)$$

where σ_x and σ_z are the Pauli matrices and the characteristic wave vector k_{so} depends on the quantum well thickness, the electron band mass and the bulk coupling constant γ : $k_{so} = \frac{m}{\hbar} \left(\frac{\pi}{d} \right)^2 \gamma$. The state functions are written as two rows single column matrices

$$\Psi(x, z, t) = \begin{pmatrix} \psi_1(x, z, t) \\ \psi_2(x, z, t) \end{pmatrix}. \quad (3)$$

The simulations that we performed were based on the time dependent Schrödinger equation

$$\Psi(t + dt) = \Psi(t - dt) - \frac{2i}{\hbar} H(t) \Psi(t) dt. \quad (4)$$

For moving electron wave packet the electrostatic potential must be evaluated in each time step which introduces the time dependence of the Hamiltonian (1) entering into Eq. (4). In each simulation as the initial condition we take a stationary eigenstate

$$H(x, z, 0) \Psi(x, z, 0) = E \Psi(x, z, 0) \quad (5)$$

with the potential distribution corresponding to a standing electron packet.

Below we apply ZnTe data parameters, in which the Dresselhaus constant is equal to $\gamma = 13.3 \text{ eV } \text{Å}^3$, the electron effective mass $m = 0.2$ and the dielectric constant $\epsilon = 7.4$. In this material the self-focusing effect is stronger than in GaAs [13] due to larger effective mass and smaller dielectric constant. The Dresselhaus coupling leads to rotation of the spin of the electron following a straight line around the direction parallel to the electron trajectory. The rotation angle depends on the distance traveled by the electron and not on duration of the motion. The rotation over a full angle occurs for the spin precession length $\lambda_{so} = \frac{\pi}{k_{so}}$. Let us assume that the electron runs in the x direction and in time t travels the distance $w(t)$. Then, its spin is rotated around the x axis by the angle $\phi(t) = 2\pi \frac{w(t)}{\lambda_{so}}$. The spin initially parallel to the z axis ($\phi(0) = 0$) after rotation by the ϕ angle becomes parallel to $\vec{\tau}(\phi) = (0, \sin(\phi), \cos(\phi))$ vector. The spin projection operator on the $\vec{\tau}$ direction is expressed by the matrix operator

$$\sigma = \vec{\tau} \cdot \vec{\sigma} = \begin{pmatrix} \cos(\phi) & -i \sin(\phi) \\ i \sin(\phi) & -\cos(\phi) \end{pmatrix}. \quad (6)$$

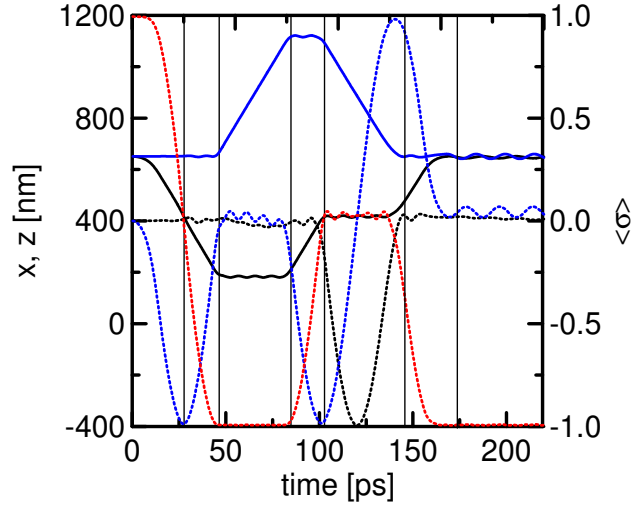


Figure 2. Results of simulations for the NOT gate. Solid lines: black and blue show the average values of $\langle x \rangle$ and $\langle z \rangle$ coordinates of the wave packet, respectively. Dotted lines: black, blue and red show the average values of the Pauli matrix operators $\langle \sigma_x \rangle$, $\langle \sigma_y \rangle$ and $\langle \sigma_z \rangle$. The solid vertical lines separate the time intervals in which the spin is subject to subsequent operations: $U_x(\phi)$, $U_x(-\pi/2)$, $U_z(\pi)$, $U_x(\pi/2)$, $U_z(-\pi)$ and $U_x(-\phi)$.

The eigenequation for this operator

$$\sigma\chi_{\pm} = \pm\sigma_{\pm} \quad (7)$$

is solved by the eigenvectors

$$\chi_{+} = \frac{1}{\sqrt{2}} \begin{pmatrix} \sqrt{1 + \cos(\phi)} \\ \frac{i \sin(\phi)}{\sqrt{1 + \cos(\phi)}} \end{pmatrix}, \quad \chi_{-} = \frac{1}{\sqrt{2}} \begin{pmatrix} \frac{i \sin(\phi)}{\sqrt{1 + \cos(\phi)}} \\ \sqrt{1 + \cos(\phi)} \end{pmatrix}. \quad (8)$$

The operator transforming the basis of eigenstates of σ_z to the above basis has the form

$$U_x(\phi) = \begin{pmatrix} \sqrt{1 + \cos(\phi)} & \frac{i \sin(\phi)}{\sqrt{1 + \cos(\phi)}} \\ \frac{i \sin(\phi)}{\sqrt{1 + \cos(\phi)}} & \sqrt{1 + \cos(\phi)} \end{pmatrix}. \quad (9)$$

Similarly one obtains the operator of the spin rotation around the z axis for the electron moving along the z axis

$$U_z(\phi) = \begin{pmatrix} 1 & 0 \\ 0 & \exp(i\phi) \end{pmatrix}. \quad (10)$$

One can also derive the operator of the spin rotation around the y axis

$$U_y(\phi) = \begin{pmatrix} \sqrt{1 + \cos(\phi)} & \frac{\sin(\phi)}{\sqrt{1 + \cos(\phi)}} \\ \frac{-\sin(\phi)}{\sqrt{1 + \cos(\phi)}} & \sqrt{1 + \cos(\phi)} \end{pmatrix}. \quad (11)$$

In contrast to U_z and U_x the U_y operator is not associated with the time evolution of the spin, but it is still useful for the system of reference transformations.

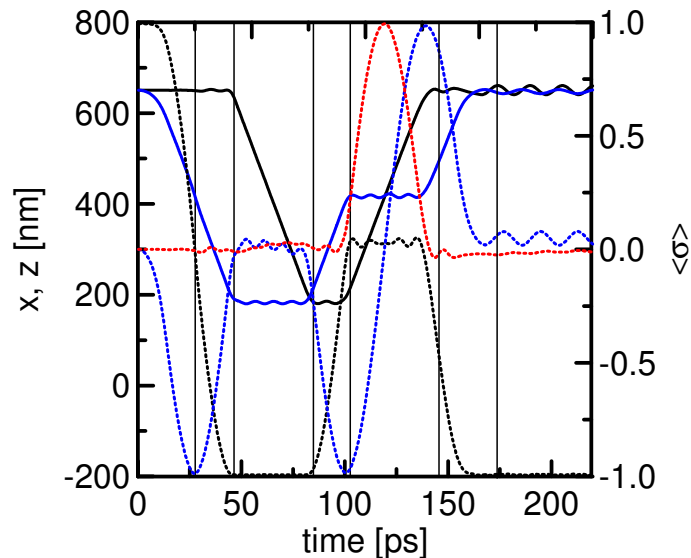


Figure 3. Same as Fig. 2 but for the phase shift gate U^π . The solid vertical lines separate the time intervals in which the spin is subject to subsequent operations: $U_z(\phi)$, $U_z(-\pi/2)$, $U_x(-\pi)$, $U_z(\pi/2)$, $U_x(\pi)$ and $U_z(-\phi)$.

3. Nanodevice

In the device based on induced quantum wires the electron packet follows any desired trajectory and consequently one can obtain an arbitrary spin rotation. For this purpose induced dots and wires [11, 12] can be used. In Fig. 1 the system of the electrodes on top of the structure is presented. In this device the spin operation will be performed for small voltages applied to the gates. The system contains 13 electrodes serving to various purposes. A small electrode e_1 plotted with the darkest shade of grey localized in the center of the device generates a quantum dot underneath it. The spin of the electron confined in this quantum dot will store the quantum bit, on which the logical operations will be performed. Pairs of electrodes (e_2, e_3) , (e_4, e_{10}) and (e_9, e_{12}) or their parts which are marked in Fig. 2 with medium grey shade are used to set the electron in

motion along closed loops. During the electron motion its spin undergoes time evolution corresponding to the logical gates: Hadamard, NOT and phase shift π gate. Parts of electrodes e_4 and e_9 marked with lighter shade of grey serve to deliver the electron from the quantum dot to the NOT or π gates. The electrodes plotted with the lightest grey are auxiliary and serve only to symmetrize the induced potential in order to make the electron trajectory as straight as possible.

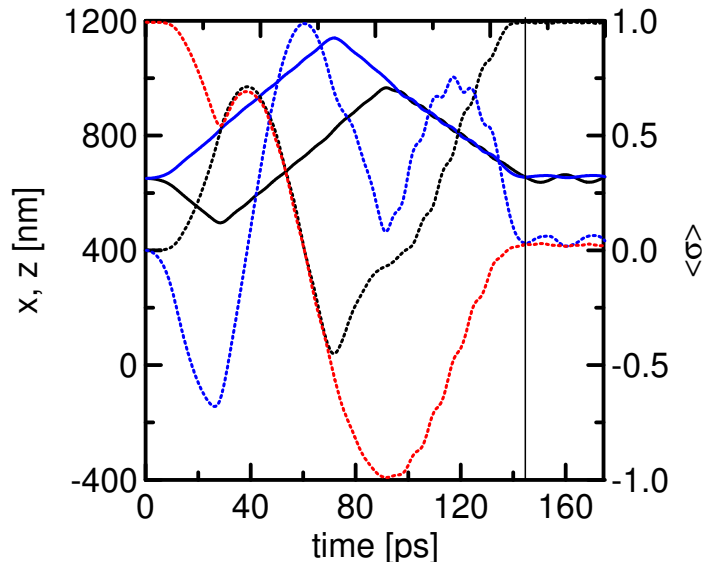


Figure 4. Same as Figs. 2 and 3 but for the Hadamard gate U^H .

The vertically oriented rectangle on the left part of the Figure composed of the e_{10} electrode and the darker part of e_4 electrode form the NOT gate. The electron going along the shorter side passes a distance of $-\lambda_{so}/4$. Its spin is rotated around the x axis by $-\pi/2$ angle, the $U_x(-\pi/2)$ operation is performed on the spin state. At the end of the segment parallel to the x axis there is a cut electrode corner [11]. The electron packet is reflected of the cur corner under a right angle and starts to move parallel to the z axis on a distance of $\lambda_{so}/2$ with the $U_z(\pi)$ operator acting on the spin state. Then the electron moves along the x and $-z$ directions with $U_x(-\pi/2)$ and $U_z(-\pi)$ operators acting on the spin state. Assembling all the spin rotations we obtain the NOT transformation

$$U = U_z(-\pi)U_x(\pi/2)U_z(\pi)U_x(-\pi/2) \quad (12)$$

$$= \frac{1}{\sqrt{2}} \begin{pmatrix} 1 & -i \\ -i & 1 \end{pmatrix} \begin{pmatrix} 1 & 0 \\ 0 & -1 \end{pmatrix} \frac{1}{\sqrt{2}} \begin{pmatrix} 1 & i \\ i & 1 \end{pmatrix} \begin{pmatrix} 1 & 0 \\ 0 & -1 \end{pmatrix} \quad (13)$$

$$= -i \begin{pmatrix} 0 & 1 \\ 1 & 0 \end{pmatrix} = U^{NOT} \quad (14)$$

The electron is delivered to the NOT gate from under the electrode e_1 along the quantum wire induced under the lighter part of the electrode e_4 . We find that for the NOT gate the length of the e_4 electrode is arbitrary, since the rotation of the spin along is compensated by the one occurring for the electron going back to the quantum dot

$$U_x(\phi)U^{NOT}U_x(-\phi) = U^{NOT}. \quad (15)$$

4. Results

In the proposed device the operations on the electron spin are induced by voltages applied to the electrodes. The subsequent steps of the spin operations can be followed at Fig. 2 in which one can observe the time dependence of the position of the center of mass of the wave packet and the average values of the Pauli matrices. The electron trajectory in the NOT gate is depicted in Fig. 1 by the black color. At the initial moment the same voltage of -0.2 mV is applied to all the electrodes. The electron is localized under the e_1 electrode with the spin set (almost) parallel to the z axis ($s_z \simeq +\hbar/2$). The NOT operation on the electron spin is performed by application of zero voltage to e_4 , e_{10} and e_{11} electrodes. The electron is first attracted to under e_4 electrode, starts to move parallel to the x axis and initially increases its velocity until the entire packet is transferred under e_4 , when the velocity becomes constant and the motion of the packet acquires a ballistic character. The electron goes to under e_{10} electrode from below the lighter part of e_4 electrode and goes around the loop. At $t = 100$ ps, when the electron is found at the uppermost electrode e_4 part, we decrease the voltage on e_{10} and e_{11} to -0.4 mV to make the electron reflect on the cut corner and leave the gate changing its direction to parallel to the x axis in order to complete the full loop. When the electron returns to under e_1 electrode, with the voltage applied to this gate being lower than the e_4 voltage, it loses its velocity and when it stops at $t = 175$ ps, we raise the voltage of e_1 to 0.1 mV to trap the electron underneath. In Fig. 2 we notice oscillations of the trapped electron position. They do not influence the electron spin that acquires orientation opposite to the z axis direction, accordingly to the NOT gate operation.

The phase shift operation is performed in exactly analogical way for the electron completing the loop along the rectangle of electrodes placed at the bottom of the device. The entire operation on the electron spin is performed by assembling separate rotations

$$U = U_z(-\phi)U_x(\pi)U_z(\pi/2)U_x(-\pi)U_z(-\pi/2)U_z(\phi) = i \begin{pmatrix} 1 & 0 \\ 0 & -1 \end{pmatrix} = U^\pi. \quad (16)$$

The phase shift π operation is performed for voltages e_9 , e_{12} and e_{13} set to zero at $t = 0$. For $t = 100$ ps the voltage on electrodes e_{12} and e_{13} is lowered to -0.4 mV to make the electron change its direction and to return to e_1 below e_9 electrode. Then for $t = 175$ ps the electron is stopped by the voltage on e_1 raised to 0.1 mV. The details of the time evolution of the position and spin can be followed in Fig. 3. This time we deliver the electron to the gate along the electrode parallel to the z direction since for the π gate the length of the segment parallel to the z direction is indifferent $U_z(\phi)U^\pi U_z(-\phi) = U^\pi$.

The last rectangle of electrodes in Fig. 1 is rotated with respect to the NOT gate by $\pi/4$ around the y axis. This rotation corresponds to the operator

$$U_y(\pi/4) = \frac{2^{-3/4}}{\sqrt{1 + \sqrt{2}}} \begin{pmatrix} 1 + \sqrt{2} & 1 \\ -1 & 1 + \sqrt{2} \end{pmatrix}. \quad (17)$$

For the electron moving around the rotated structure the spin is manipulated as

$$U = U_y^\dagger(\pi/4)U^{NOT}U_y(\pi/4) = \frac{1}{\sqrt{2}} \begin{pmatrix} 1 & 1 \\ 1 & -1 \end{pmatrix} = U^H, \quad (18)$$

in which we recognize the Hadamard transform. For the Hadamard gate zero voltage is set to e_3 . The electron is extracted to under e_3 from under e_1 . When the electron acquires a velocity at $t = 30$ ps we put zero the voltage on e_2 and after the electron returns to under e_1 its voltage is raised to 0.1 mV. The results of simulations are presented in Fig. 4. Electron with spin initially set parallel to the z axis goes to the state in which it is parallel to the x axis, i.e. to an even superposition of states parallel and antiparallel to the z axis. In the proposed nanodevice the Hadamard operation is accomplished in the shortest time since e_1 is placed at the corner of the rectangle and the electron does not need to be delivered from e_1 to the gate.

5. Summary and Conclusion

The self-focusing effect due to the interaction of the electron packet with the charge induced on the electrodes placed on the surface of the semiconductor nanostructure allows for the electron transfer along a designed trajectory between chosen points in the device in form of a wave packet of a stable shape. In a semiconducting material in which the spin-orbit coupling is present the electron motion is accompanied by rotation of its spin by the angle which depends on the direction of motion and the distance traveled. For carefully chosen lengths of the segments one can assemble the rotation into basic single qubit operations. For electrodes forming closed loops with a common quantum dot at the beginning and the end of each electron loop one can apply the quantum gates sequentially in an arbitrary order. The nanodevice proposed in the present paper is designed to perform any sequence of operation of the most popular single qubit gates: NOT, Hadamard and phase shift. The choice of the operation and its implementation requires application of weak DC voltages. The performed computer simulations were obtained by iterative solution of the time dependent Schrödinger equation. The presented results contained the time evolution of the position and spin of the electron and their related modifications. The simulations indicate that the operations designed algebraically can indeed be performed. For the numerical calculations the material data of a specific material (ZnTe). The proposed device has dimensions which are realistic and can be produced by the present technology. Therefore, both the processes of the spin rotations and the obtained operation times are reliable.

References

- [1] S. Datta and B. Das, *Appl. Phys. Lett.* **56**, 665 (1990).
- [2] D. Awschalom, D. Loss, and N. Samarth, *Semiconductor Spintronics and Quantum Computation*, Springer Verlag, Berlin, 2002.
- [3] R. Hanson, L.P. Kouwenhoven, J.R. Petta, S. Tarucha, and L.M.K. Vandersypen, *Rev. Mod. Phys.* **79**, 1217 (2007).
- [4] J. M. Elzerman, R. Hanson, L. H. Willems van Beveren, B. Witkamp, L. M. K. Vandersypen and L. P. Kouwenhoven, *Nature* **430**, 431 (2004).
- [5] T. Meunier, I.T. Vink, L.H. Willems van Beveren, F.H.L. Koppens, H.P. Tranitz, W. Wegscheider, L.P. Kouwenhoven, and L.M.K. Vandersypen, *Phys. Rev. B* **74**, 195303 (2006).
- [6] J.R. Petta, A.C. Johnson, J.M. Taylor, E.A. Laird, A. Yacoby, M.D. Lukin, C.M. Marcus, M.P. Hanson, A.C. Gossard, *Science* **309**, 2180 (2005).
- [7] F.H.L. Koppens, C. Buizert, K.J. Tielrooij, I.T. Vink, K.C. Nowack, T. Meunier, L.P. Kouwenhoven and L.M.K. Vandersypen, *Nature* **442**, 766 (2006).
- [8] K.C. Nowack, F.H.L. Koppens, Yu.V. Nazarov, and L.M.K. Vandersypen, *Science* **318**, 1430 (2007).
- [9] P. Foeldi, B. Molnar, M.G. Benedict, and F. Peeters, *Phys. Rev. B* **71**, 033309 (2005).
- [10] P. Foeldi, O. Kalman, M. G. Benedict, and F. Peeters, *Phys. Rev. B* **73**, 155325 (2006).
- [11] S. Bednarek, B. Szafran, R. J. Dudek, and K. Lis, *Phys. Rev. Lett.* **100**, 126805 (2008).
- [12] S. Bednarek and B. Szafran, arXiv:0807.1627.
- [13] S. Bednarek, B. Szafran, and K. Lis, *Phys. Rev. B* **72**, 075319 (2005).
- [14] S. Bednarek and B. Szafran, *Phys. Rev. B* **73**, 155318 (2006).
- [15] G. Dresselhaus, *Phys. Rev.* **100**, 580 (1955).
- [16] E.I. Rashba, *Sov. Phys. Solid State* **2**, 1109 (1960).